Collisional transport in a low aspect ratio tokamak

D. A. Gates, H. E. Mynick, and R. B. White
Plasma Physics Laboratory, Princeton University, P.O. Box 451, Princeton, New Jersey 08543

(Received 30 March 2004; accepted 15 June 2004; published 2 August 2004)

Calculations of collisional diffusivities in toroidal magnetic plasma confinement devices order the toroidal gyroradius to be small relative to the poloidal gyroradius, i.e., $\rho_{i_\phi} \ll \rho_{i_\theta}$, where $\rho_{i_\phi} \equiv m_i v_{th_i}/qB_\phi$ and $\rho_{i_\theta} \equiv m_i v_{th_i}/qB_\theta$. This ordering is central to what is usually referred to as neoclassical transport theory. This ordering is incorrect at low aspect ratio (with aspect ratio $A \equiv R/a$, where R is the major radius of the torus and a is the minor radius), where it can be the case that $\rho_{i_\phi} > \rho_{i_\theta}$. The correction to the test particle diffusivities is numerically calculated by comparing the diffusivities as determined by a full orbit code (which we refer to as omniclassical diffusion) with those from a gyroaveraged orbit code (neoclassical diffusion), and then corroborated by an analytic calculation. The omniclassical diffusion can be up to 2.5 times the calculated neoclassical value. The implications of this work for the analysis of collisional transport in low aspect ratio devices are discussed. © *2004 American Institute of Physics*. [DOI: 10.1063/1.1781165]

The theory of diffusion of particles across a uniform magnetic field (referred to as classical diffusion) was developed nearly 50 years ago,[1,2] but was found insufficient to explain the observed diffusion in toroidal devices. The theoretical basis of collisional transport in high aspect ratio magnetic plasma confinement devices has been well established for at least 30 years (see, e.g., Refs. 3–5). Transport theory at high aspect ratio is based on the "small gyroradius expansion," which assumes that $\rho_i/a \equiv \rho^* \ll 1$. In addition, it is generally assumed that $|B_\theta/B_\phi| \ll 1$ (where B_θ is the poloidal magnetic field and B_ϕ is the toroidal magnetic field), which is in turn the result of two additional assumptions—$\epsilon \equiv a/R < 1$ (where a is the minor radius of the torus and R is the major radius) and $q \equiv d\Phi/d\psi = O(1)$ (where Φ is the toroidal flux and ψ is the poloidal flux). In low aspect ratio tokamaks,[6] often referred to as spherical torii, the $\epsilon \ll 1$ assumption is explicitly violated. As a result, the assumption that $|B_\theta/B_\phi| \ll 1$ is also invalid. These assumptions are fundamental to the derivation of the gyroaveraged kinetic equation, also known as the drift kinetic equation. The drift kinetic equation is the basis of neoclassical transport theory.

In order to determine the magnitude of the correction to collisional transport due to finite gyroradius, we first compare the result of the gyroaverage orbit code ORBIT (Refs. 7 and 8) with those from the full orbit code GYROXY.[9] We coin the word omniclassical to refer to transport calculations based on full particle orbits in general toroidal geometry with arbitrary aspect ratio. The collision frequency and temperatures are set to be the same in both codes and the diffusivities are calculated. Care was taken to verify that the same pitch angle scattering rate was obtained in each code, due to the very different scattering operators used. It is useful to note that the actual value of the collision frequency falls out of this ratio as long as the collisionality is well into the banana regime (i.e., $\nu_{ie} \ll \omega_b$), since we are only interested in the ratio of omniclassical to neoclassical diffusion (and diffusion is linear in collision frequency). The correction is therefore essentially a geometric correction factor, arising from the now widely differing full and gyroaveraged orbits. We restrict ourselves to considering only modifications to the ion transport. In a real plasma, however, the collisionality regime may vary across the minor radius, which may modify the resultant correction factor profile. We then compare these results to an analytic theory valid for arbitrary aspect ratio. The analytic calculation is based on angular momentum conservation and is valid at arbitrary aspect ratio and β.

Two equilibria from the National Spherical Torus Experiment (NSTX) (Ref. 10) were chosen as representative low aspect ratio equilibria. Isoflux contour plots of the equilibria used are shown in Figs. 1 and 2. These particular equilibria were chosen because they have very different values of $|B_\theta/B_\phi|$, so as to determine in a rough manner how strongly the transport correction scales with this ratio. The double null discharge (equilibrium 1) has $B_\phi(0) = 0.3$ T [where $B_\phi(0) \equiv$ the applied vacuum toroidal field at the vessel midpoint, i.e., $R = 0.86$ m] and with $I_p = 1.2$ MA (where $I_p \equiv$ the toroidal plasma current), whereas the single null discharge (equilibrium 2) has $B_\phi(0) = 0.5$ T and $I_p = 0.8$ MA. The ratio of $|B_\theta/B_\phi| \sim \mu_0 I_p/(2\pi a\sqrt{1+\kappa^2}B_\phi)$ (with $\kappa = b/a$ and b the plasma height) varies more than a factor of 2 between the chosen equilibria (the relevant geometric factors vary between these discharges on the order of 10%).

Representative particle orbits are shown for equilibrium 1 in Figs. 3 and 4. The plot region in Fig. 4 is indicated by the box in Fig. 3. In Fig. 3 the black trace is the full orbit, whereas the red trace is the gyroaveraged orbit. It is evident from this picture alone that the diffusion step size will vary substantially between the two models. In Fig. 4, which has a plot region corresponding to the box drawn in Fig. 3, the black trace is the downward drifting part of the full orbit and green is the upward drifting part, whereas the red dashed line is the gyroaveraged orbit. Note that the maximum orbit width for the full orbit varies by nearly a factor of 5 over the banana width (denoted in Fig. 4 as Δ_b for the banana width and Δ_{tot} for the full orbit width).

To carry out the numerical simulations, 2000 particles

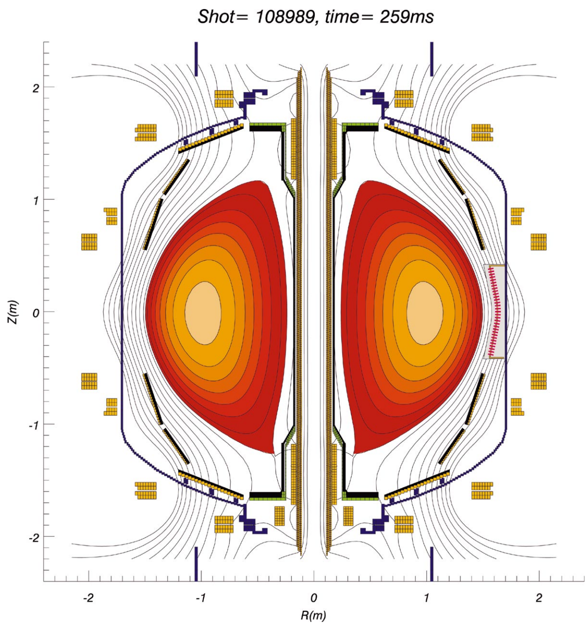

FIG. 1. (Color). Isoflux contour plot for NSTX shot number 108 989, B_{ϕ} (R=0.86 m)=0.3T, I_p=1.2 MA, β_t=35%.

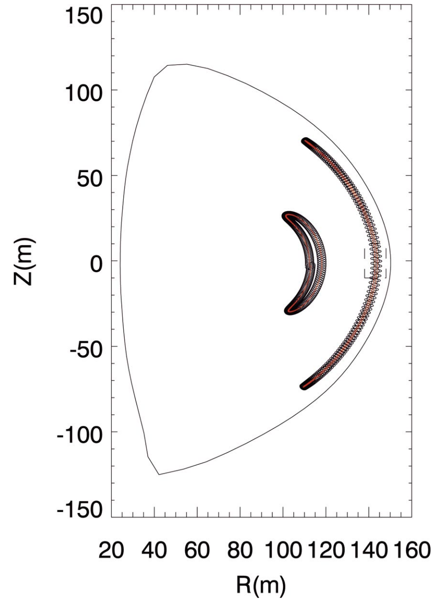

FIG. 3. (Color). Representative calculated particle orbits for the full orbit code (black) and the gyroaveraged orbit code (red) for the equilibrium in Fig. 1. The particle has E=2.0 keV, $\lambda_0 = v_{\|_0}/v = 0.3$. The inner particle is born on the flux surface located at R=115 cm, Z=0 cm, while the outer orbit is born at R=145 cm, Z=0 cm.

with energy 1.1 keV are deposited as a δ function in ψ with uniform poloidal distribution, but with a random initial velocity space pitch angle distribution. This distribution is then allowed to evolve under the influence of pitch angle scattering and, for the full orbit code, gyrophase scattering. The effect of energy scattering is ignored, an assumption that permits simplification of both the numerical and analytical calculation. The effect of energy scattering on diffusivity will be the topic of future work. The mean square normalized flux deviation from the initial flux surface is plotted vs time for equilibrium 1 for the flux surface with an outboard major

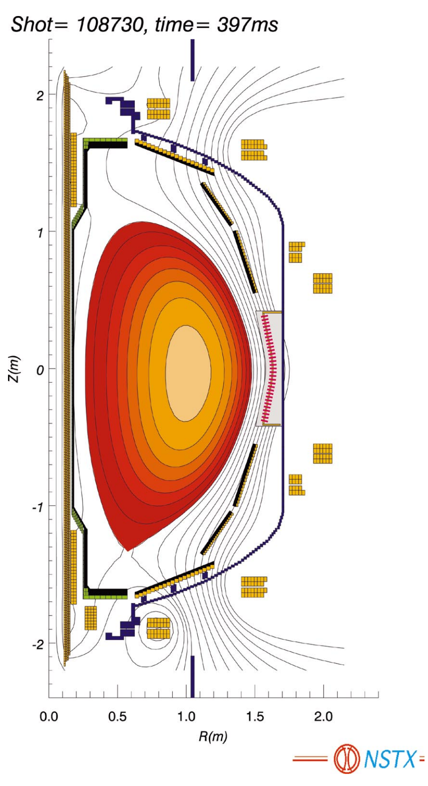

FIG. 2. (Color). Isoflux contour plot for NSTX shot number 108 730, B_{ϕ} (R=0.86 m)=0.45 T, I_p=0.8 MA, β_t=15%.

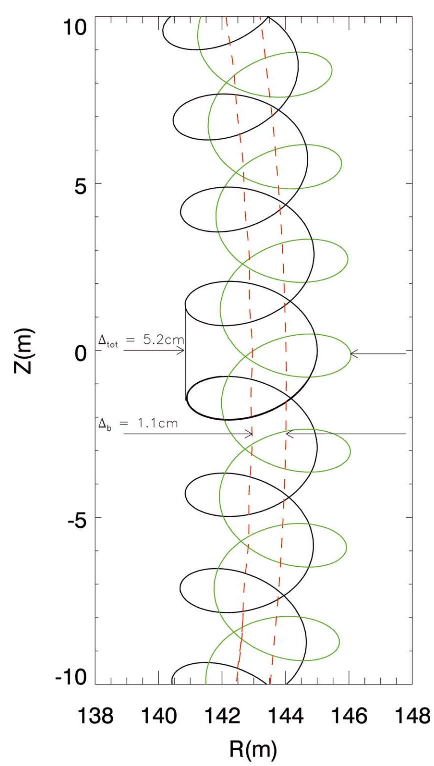

FIG. 4. (Color). Expanded view of the orbits in Fig. 3 (the plot region corresponds to the region of the box shown in Fig. 3). Notice the large difference between the maximum orbit widths for the full orbit, Δ_{tot}, and the gyroaveraged orbit Δ_b.

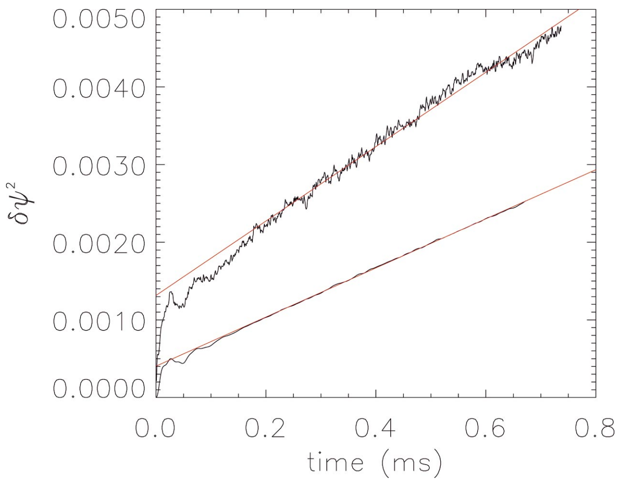

FIG. 5. (Color). Time history of the mean square deviation from the starting flux surface measured in units of normalized flux. The red line is a least squares fit to the data after $t=0.15$ ms. The slope of this line is the particle diffusivity in flux space.

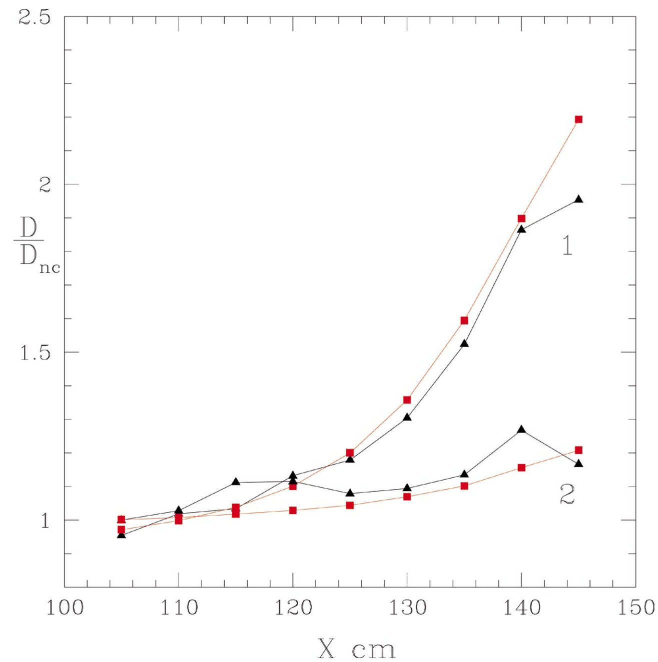

FIG. 6. (Color). Radial profiles of the diffusivity correction factor due to finite gyroradius for the two equilibria above. Black lines are for the numerical calculation and red lines are for the analytical calculation.

radius located at $R=130$ cm in Fig. 5 for both the neoclassical and the full omniclassical case. After filling in the orbit widths from the initial δ-function distribution (typically in one to two bounce times) the particles then diffuse radially. A line is fitted to each time sequence, the slope of which is the diffusivity and the offset is the mean orbit width in flux coordinates.

The calculation is then repeated at ten flux surfaces which are equally spaced in outboard major radius, one every 5 cm starting at $R=110$ cm (thereby avoiding both the magnetic axis and the last closed flux surface). Checks of the variation of the diffusivity with collisionality in the banana regime indicate that the dependence is linear with unity slope to better than 5%. Checks were also performed with analytic high aspect ratio equilibria to verify that the omniclassical to neoclassical diffusivity ratio approaches 1 at high aspect ratio and that the neoclassical high aspect ratio result is in agreement with analytic diffusion coefficients as given in, for example, Ref. 11. Also, we verified that the ratio of omniclassical to neoclassical (test particle) thermal diffusivity is the same as the equivalent ratio for the particle diffusivities to a high degree of accuracy (thermal diffusivity is calculated using a Maxwellian initial energy distribution and weighting the square of the displacement with energy).

The resultant omniclassical to neoclassical diffusivity ratio is plotted vs normalized poloidal flux for both equilibria 1 and 2 in Fig. 6. The peak ratio is $\sim$2.5, for the higher current low toroidal field case (equilibrium 1). The higher field lower current equilibrium (equilibrium 2) also has a small correction over the neoclassical value with a mean value of $\sim$1.1. The omniclassical to neoclassical diffusivity ratio rises strongly with radius for equilibrium 1, while for equilibrium 2 the peak correction factor is more flat. Equilibrium 1 is a paramagnetic plasma, so the toroidal field falls off faster than $1/R$, whereas equilibrium 2 is nearly diamagnetic giving rise to a smaller variation in toroidal field as R increases.

Also shown in Fig. 6 are the results of an analytic calculation of the test particle diffusion, using a method similar to that described in Ref. 12, but using a simplified integrability condition. The focus of Ref. 12 was not low aspect ratio, and assumed expressions for the radial fluxes were valid only for very low β. The analytic expression represented in Fig. 6 is valid for high β. The analytic calculation indicates that the correction to neoclassical arises from the appropriate generalization of classical transport to this low aspect ratio geometry. Omniclassical diffusion can therefore be thought of as the sum of classical and neoclassical diffusion when the two terms are of the same order.

The effect of finite gyroradius at low aspect ratio has been investigated previously[13] for slowing down of fast (neutral beam) particles. In this work, the effects of finite gyroradius on diffusion were ignored, since the slowing down rate is typically larger than the pitch angle scattering rate for fast ions. The result of this work was that the gyroaveraged orbit model was sufficient for modeling fast particle slowing down (i.e., for calculating plasma heating from fast particles). The reason that diffusion is not well represented by gyroaverage orbits, while slowing down is, can be simply understood. On average the region over which a particle will deposit its energy is centered about the mean location of the particle. Since the gyroorbit is still roughly circular, the average particle location is still very near the location of the gyroaveraged orbit (accurate to within the approximation that the field does not vary over the gyroradius, i.e., the $\rho_{i_\phi}/a \ll 1$). Diffusivity, on the other hand, scales as $\chi \sim \nu_{\text{eff}}\rho_{\text{eff}}^2$ where ρ_{eff} is a measure of the rms deviation of a particle from a flux surface and ν_{eff} is the effective pitch angle scattering rate. However, as is apparent from Fig. 4, the rms deviation from a flux surface varies significantly between the full and gyroaveraged orbits.

An important implication of this work is that the omniclassical ion test particle transport is measurably higher than predicted by neoclassical theory. This is particularly important given recent experimental results from NSTX that have shown measured ion temperatures well in excess of those predicted by neoclassical theory as calculated by the NCLASS code[14] (see Ref. 15 for NSTX results). (The ratio of test particle diffusivities can be considered an approximation for the ratio of ion thermal diffusivities.) The omniclassical corrections calculated above motivates the reexamination of the theoretically predicted ion temperature for the plasmas given in Ref. 15 (equilibrium 2 is in fact the same equilibrium for which the neoclassical ion temperature was calculated in Ref. 15). This will increase the magnitude of the apparent ion temperature anomaly by widening the gap between the predictions of the maximum possible ion temperature and those measured in the experiment. This expected increase in omniclassical thermal diffusivity therefore strengthens the argument for the possible existence of an additional ion heat source in low aspect ratio tokamaks heated by neutral beams (see, e.g., Ref. 16). Similarly, comparisons to neoclassical theory in other spherical torus devices such as the small tight aspect ratio tokamak bear reexamination.[17] A detailed comparison to experimental data will require a more complete theory of omniclassical transport, including electric field effects and energy scattering as well as multispecies effects. Finally, we note that the ORBIT and GYROXY results for bootstrap current are in close agreement, consistent with what one expects from analytic theory.

ACKNOWLEDGMENTS

The authors would like to acknowledge helpful discussions with D. R. Mikkelsen.

This work was supported by the U.S. Department of Energy Grant under Contract No. DE-AC02-76CH03073.

[1] C. L. Longmire and M. N. Rosenbluth, Phys. Rev. **103**, 507 (1956).
[2] M. N. Rosenbluth and A. N. Kaufman, Phys. Rev. **109**, 1 (1958).
[3] F. L. Hinton and R. D. Hazeltine, Rev. Mod. Phys. **48**, 239 (1976).
[4] M. N. Rosenbluth, R. D. Hazeltine, and F. L. Hinton, Phys. Fluids **15**, 116 (1972).
[5] A. H. Glasser and W. B. Thompson, Phys. Fluids **16**, 95 (1973).
[6] Y-K. M. Peng and D. J. Strickler, Nucl. Fusion **26**, 769 (1986).
[7] R. B. White and M. S. Chance, Phys. Fluids **27**, 2455 (1984).
[8] R. B. White, Phys. Fluids B **2**, 845 (1990).
[9] R. B. White, L. Chen, and Z. Lin, Phys. Plasmas **9**, 1890 (2002).
[10] M. Ono, S. M. Kaye, Y.-K. M. Peng *et al.*, Nucl. Fusion **40**, 557 (2000).
[11] A. A. Galeev and R. Z. Sagdeev, JETP Lett. **26**, 223 (1968).
[12] P. H. Rutherford, Phys. Fluids **13**, 482 (1970).
[13] D. R. Mikkelsen, R. B. White, R. J. Akers, S. M. Kaye, D. C. McCune, and J. E. Menard, Phys. Plasmas **4**, 3667 (1997).
[14] W. A. Houlberg, K. C. Shaing, S. P. Hirshman, and M. C. Zarnstorff, Phys. Plasmas **4**, 3230 (1997).
[15] D. A. Gates and the NSTX national research team, Phys. Plasmas **10**, 1659 (2003).
[16] D. A. Gates, N. N. Gorelenkov, and R. B. White, Phys. Rev. Lett. **87**, 205003-1 (2001).
[17] D. A. Gates, R. Akers, L. Appel *et al.*, Phys. Plasmas **5**, 1775 (1998).